

# We are IntechOpen, the world's leading publisher of Open Access books Built by scientists, for scientists

4,800

Open access books available

122,000

International authors and editors

135M

Downloads

Our authors are among the

154

Countries delivered to

TOP 1%

most cited scientists

12.2%

Contributors from top 500 universities



WEB OF SCIENCE™

Selection of our books indexed in the Book Citation Index  
in Web of Science™ Core Collection (BKCI)

Interested in publishing with us?  
Contact [book.department@intechopen.com](mailto:book.department@intechopen.com)

Numbers displayed above are based on latest data collected.  
For more information visit [www.intechopen.com](http://www.intechopen.com)



# Anodic ZnO-Graphene Composite Materials in Lithium Batteries

*Herrera-Pérez Gabriel, Pérez-Zúñiga Germán,  
Verde-Gómez Ysmael, Valenzuela-Muñiz Ana María  
and Vargas-Bernal Rafael*

## Abstract

An important area to cope with in the implementation of technologies for the generation of energy from renewable sources is storage, so it is a priority to develop new ways of storing energy with high efficiency and storage capacity. Experimental reports focused on ZnO-graphene composite materials applied to the anode design which indicated that they show low efficiencies of around 50 %, but values very close to the theoretical capacity have already been reported in recent years. The low efficiency of the materials for the anode design of the Li-ion battery is mainly attributed to the pulverization and fragmentation of the material or materials, caused by the volumetric changes and stability problems during the charge/discharge cycles. In this chapter, we will discuss the development of composite materials such as ZnO-graphene in its application for the design of the anode in the Li-ion battery.

**Keywords:** ZnO, batteries, graphene, Li-ion, composites, ZnO-Graphene

## 1. Introduction

The search for new and efficient energy storage systems has been mainly aimed at batteries, which have positioned themselves as one of the best options for this purpose [1]. The development and innovation in such systems has been slow compared to other technologies since the relevant innovations have taken even centuries, from the invention of the battery in 1800 by Alessandro Volta [2], then the first lead-acid batteries partially rechargeable in 1860 by Gaston Planté [3], up to the lithium-ion batteries, which Sony introduced to the market in 1991 [4].

The batteries can be classified as primary (not rechargeable) and secondary (rechargeable). The classification of the batteries is made in relation to the active materials, in the components of the battery. At present, there are still few batteries with the ability to have reversible electrochemical reactions. **Table 1** shows some of the main physical and chemical properties of current commercial batteries. The Li-ion batteries, clearly positioned today, as one of the best options for energy storage, are far above the other batteries in terms of the number of cycles.

### 1.1 Overview of batteries

The first Li-based batteries used  $\text{LiCoO}_2$  cathode, anode carbon, and  $\text{LiPF}_6$  electrolytes, with a capacity of around 140 mAh and 3.7 V and an efficiency of 50 %,

Battery type	Anode	Cathode	Electrolyte	Voltage (V)	Duration (cycles)
Li-ion	Graphite	LiCoO <sub>2</sub>	LiPF <sub>6</sub> (nonaqueous)	3.7	>1000
Pb-acid	Pb	PbO <sub>2</sub>	H <sub>2</sub> SO <sub>4</sub> (aqueous)	2.1	<500
Ni-Cd	Cd	NiOOH	KOH(aqueous)	1.2	2000
NMH	Ti <sub>2</sub> Ni+TiNi	NiOOH	KOH(aqueous)	1.2	500–1000

**Table 1.**  
General characteristics of the most commonly used commercial batteries [5].

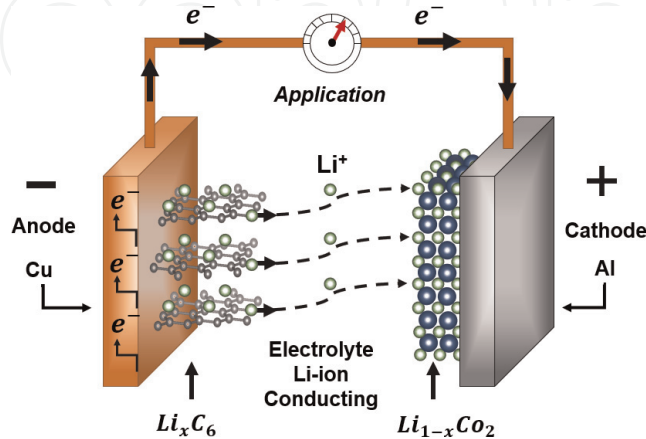


**Figure 1.**  
Schematic of a Li-ion cell.

which was relatively low. The innovations that followed in the Li-ion batteries revolved around the three main components that are the anode, cathode, and electrolyte, in order to improve the characteristics and problems that currently accompany this technology, such as the capacity of gravimetric and volumetric power, safety, cost, efficiency, and the search for materials that do not harm the environment [4, 6, 7].

A Li-ion battery is a set of cells, connected in series or in parallel in **Figure 1**. A diagram of the main components of a Li cell is shown, which are a negative electrode or anode and the positive electrode or cathode and between them a Li-ion conductive electrolyte. The principle of the operation of a cell is based on the transport of Li-ions between the two electrodes, capable of storing Li [1].

During the charge and discharge processes, the electrons flow from the anode to an external load and to the cathode in a discharge process, through an oxidation reaction at the anode and a flow of Li-ions from the anode to the cathode through the electrolyte. In a charging process, the flow of electrons is from the cathode to a source and to the anode, followed by a reduction reaction at the cathode and a flow of Li-ion to the anode through the electrolyte, forming a circuit. The collectors of charge or substrates that are used regularly are copper and aluminum for the anode and cathode, respectively [8].

The standard potential of a cell is determined by the type of active materials in the cell and can be calculated in relation to the Gibbs free energy or obtained experimentally. This potential can be calculated from the standard potential of the electrodes in the following way:

$$\text{anode (oxi.potential)} + \text{cathode (red.potential)} = \text{standard cell potential} \quad (1)$$

The oxidation potential is the negative value of the reduction potential; it is worth mentioning that it is dependent on other factors such as concentration and

temperature. The theoretical capacity of a cell is determined by the amount of active materials; this expresses the amount of electricity involved in the electrochemical reaction, which can be expressed in terms of coulombs or ampere/hour [8].

## 1.2 Materials for the design of electrodes

Within the characteristics of the electrodes, two phenomena mainly occur: diffusion and adsorption. The diffusion phenomenon happens in the cathode, and the carbon that is commonly used in the anode presents a phenomenon of adsorption. Nowadays the diversity of existing materials that are used or that are proposed for the electrodes and the great majority are governed by diffusion phenomena or in a composite material (CM) in which both phenomena are involved [9].

The first Li-ion batteries had been based on components as  $\text{LiCoO}_2$  electrodes in the cathode and carbon in the anode. The development and innovation in the components of a rechargeable battery have considerably improved characteristics, such as the capacity of gravimetric and volumetric power, which has led to the development of batteries with equal or greater power but of lower weight and volume [6].

### 1.2.1 Cathode

A wide variety of materials has been used for the cathode since the introduction of the first Li-ion batteries. Specifically, Li-ion batteries are not governed by the chemical potentials of the materials involved, so the  $\text{Li/Li}^+$  potential for both electrodes is taken as a reference. This means that the material of the cathode that will interact with the Li must have a high potential (+) in relation to that of  $\text{Li/Li}^+$  [8, 9].

One of the most significant innovations that was made in the first batteries was the replacement of the Co, which was expensive and also toxic, being replaced by the Mn, which significantly decreased the price and at the same time increased the power capacity to  $250 \text{ mAhg}^{-1}$  and a voltage of 4.6–2.5 V [6]. After the innovation that occurred with the  $\text{LiMn}_2\text{O}_4$ , new proposals like  $\text{LiFePO}_4$  [10] were developed, and recently high ionic conductivity systems were investigated, in which the S is mainly involved, which has a theoretical capacity of  $1675 \text{ mAhg}^{-1}$  [6].

### 1.2.2 Anode

The graphite that was used in the first Li-ion batteries had a capacity that was theoretically limited to  $372 \text{ mAhg}^{-1}$  [4], and as a solution to these limitations, various materials have emerged such as Si, Sn, Sb, Ge, and new forms allotropic carbon [11]. The materials used at the anode, unlike the cathode, must have a potential no greater than that of  $\text{Li/Li}^+$  and less than the potential of the cathode. That is, the materials that are used as electrodes should not have a greater potential than  $\text{Li/Li}^+$  since the Li-ions could be reduced by forming metallic Li and in certain circumstances dendrites that considerably reduce the cycles and especially generate problems of safety since they can cause short circuit, which is one of the main problems when metallic Li is used as an anode [5, 8].

In recent years, transition metal oxides (TMO) have been used, such as Ni, Sn, Mn, and Zn, among others. In a fully charged Li battery, the anode contains an excess of Li-ions that have a chemical potential to diffuse through the electrolyte and into the vacancies of the cathode structure [5]. **Figure 2** shows a representative diagram of a charging and discharging process for a Li battery, and as can be seen

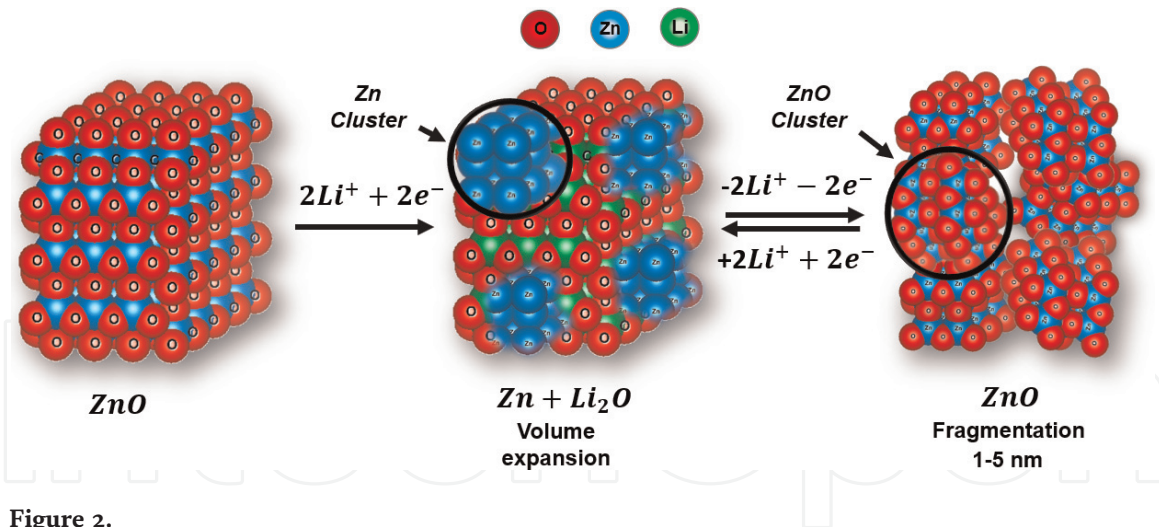
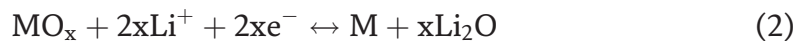


**Figure 2.**  
Reversible conversion reaction of an metallic oxide (MO) with Li.

during the lithiation process, the metallic oxide (MO) is reduced to its metallic state, inside a  $Li_2O$  matrix according to the following reaction:



In the lithiation process, metal nanoparticles (M) embedded in a  $Li_2O$  matrix are formed (this generates volumetric expansion), and in the first discharge the nanoparticles of metal (M) are oxidized again into smaller particles.

Graphene is a material that in recent years has attracted a lot of attention due to its exceptional properties and its potential application in many areas, being one of them in Li-ion batteries, where it is used in the negative electrode. However, it has been seen that it cannot be used in a pure manner, because after the first discharge, it presents great problems of reversibility, so it is common for it to be widely used with other materials in a composite, generally with MO [5, 12].

## 2. Materials for the design of the ZnO-graphene system

Currently, graphene is one of the most researched and promising materials to replace graphite in Li-ion battery anode. When using graphene in an CM, it is expected to take advantage of the properties of high conductivity and high surface area, and in the specific case when used with an MO, it works as a buffer of the volumetric changes that it undergoes in lithiation [13]. One of the pioneers in the study of the intercalation of Li in various carbonaceous materials was Dahn et al. [14] where they concluded that graphite is limited to a certain amount of Li retention and that, in addition most of the processes of interaction with lithium, it is dominated by mechanisms of physical interaction.

Graphene, which is usually used as CM, usually comes from graphite and is obtained as GO. In several tests that have been carried out as anodes, irreversible capacities of up to  $1250 \text{ mAhg}^{-1}$  have been obtained in the first cycle; this is due to the formation of a solid interface with the electrolyte (SEI), which is one of the main causes of the decrease in capacity, which at the same time is due to the high surface area [5].

Carbon/metal CMs are made with metals that are capable of forming alloys with Li or transition metal oxides (TMO), a term introduced by Tarascon et al. in the year 2000 and where they show several MO reporting reversible capacities of up to  $700 \text{ mAhg}^{-1}$  [15]. One of the main disadvantages when using an MO is that they are

generally poor electrical conductors or in certain cases semiconductors, being one of the causes for which they are commonly used in CM, with carbonaceous materials that compensate for these deficiencies of conductivity and volumetric changes [5].

One of the MO that is being investigated as an anode is ZnO, which theoretically has a capacity of  $987 \text{ mAhg}^{-1}$ ; the charge and discharge reactions can be written as follows:



Complete reaction:



The theoretical capacity of ZnO can be calculated as follows:

$$\begin{aligned} C_t(\text{mAhg}^{-1}) &= (z \times F (\text{Cmol}^{-1})) / (M_w(\text{gmol}^{-1})) = \\ &= (z \times 96485 (\text{A s})) / 81.39 (\text{g}) = \\ &= (z \times 26801 (\text{mAh})) / (M_w(\text{g})) = \\ &= (3 \times 26801 (\text{mAh})) / 81.39\text{g} = 987.87 (\text{mAhg}^{-1}) \end{aligned} \quad (6)$$

where  $C_t$  is the theoretical specific capacity,  $F$  is the Faraday constant,  $z$  is the number of electrons transferred from each structural unit, and  $M_w$  is the molecular weight [16].

The theoretical capacity of ZnO is one of the reasons why this material is interesting to be used as an anode in Li-ion battery. However, it is not only of interest because of its theoretical capacity, since it is also a material that, unlike the other transition metal oxides, has certain advantages such as high chemical stability, low cost, nontoxic, and relative ease of synthesis with a large number of methods and a great variety of structures and morphologies [17–21].

## 2.1 Zinc oxide

ZnO is a material of great interest in various research areas and a large number of technological applications, such as in ceramics, piezoelectric, transducers, chemical sensors, catalysis, optical applications, photovoltaics, and lithium batteries, among many others. For this reason, the interest in this material continues to be latent since it is also one of the few oxides that shows effects of quantum confinement to certain particle sizes [22–24].

ZnO is a material with great versatility, in terms of synthesis methods and nanostructures, such as nanobars [20], nanosheets [25, 26], 3D nanostructures [27, 28], and nanocrystals [18, 29]. Within the synthesis methods, relatively complex methods are found such as the chemical vapor deposition (CVD) [30], Vapor Phase Transport (VPT) [31] for its acronym in English. These techniques are relatively expensive and complex, compared to others such as chemical precipitation [28, 32], sol-gel [23, 33–35], hydrothermal [29, 36–41], or solvothermal [19, 42, 43].

The Wurtzite phase that is defined by a hexagonal crystalline system is the most stable phase of ZnO at environmental conditions, but this ZnO can also be obtained in cubic phase forming the zinc blende; and using Si substrates and with high pressures, the rock of salt (NaCl) form is obtained. The structure of the orthorhombic unit cell of the main precursor phase of the Wurtzite, which is the Wülfingite, that chemically is  $\text{Zn}(\text{OH})_2$ , is presented in **Figure 3a, b**. For wurzite

form is presented in **Figure 3c, d** the Hexagonal crystalline system and that belongs to the space group P63mc, with the network parameters  $a = 0.35$  nm and  $c = 0.52$  nm [44]. Wurtzite is a material with a relatively simple atomic crystalline structure, in which it can be seen that each atom of Zn is surrounded by four atoms of O forming

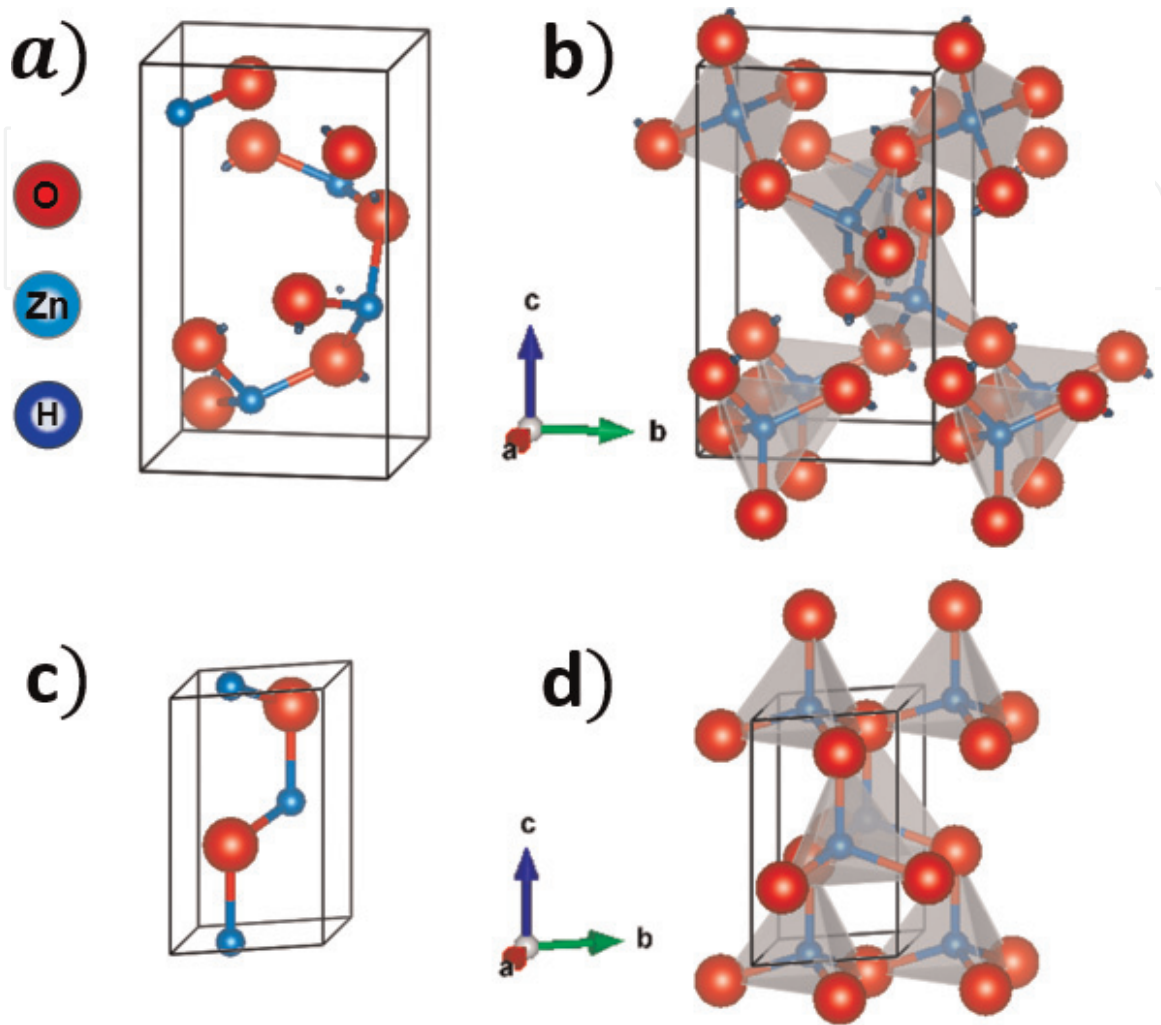


**Figure 3.** (a) Unitary cell of  $\epsilon$ - $Zn(OH)_2$ , (b) representation of polyhedra of the unitary cell of the wulfingite, (c) unitary cell of  $ZnO$ , and (d) representation of polyhedra of the unit cell of the wurtzite.

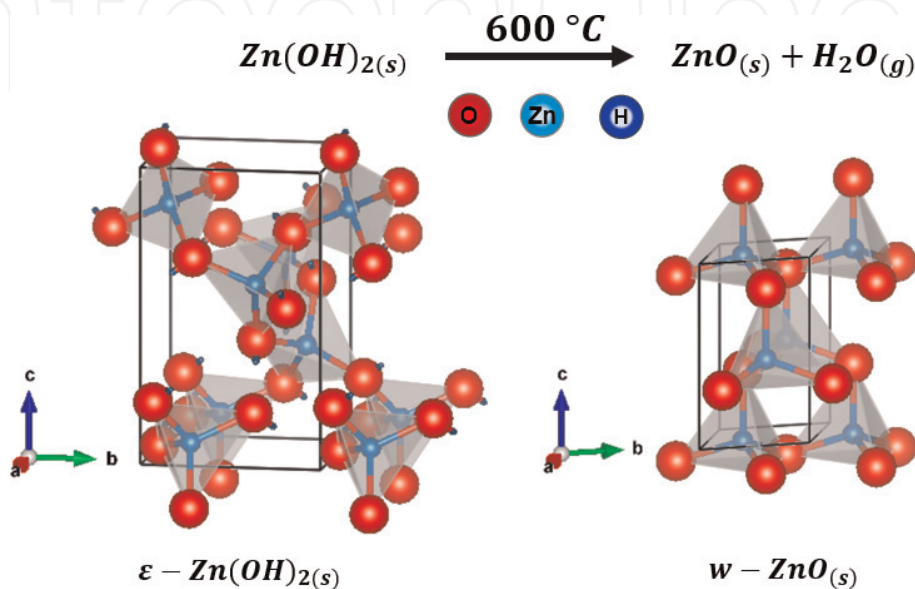


**Figure 4.** Thermal transformation of zinc hydroxide (wulfingite) for zinc oxide (wurtzite).

a tetrahedron and likewise with each atom of O surrounded by four atoms of Zn forming tetrahedral indicating the one-to-one ratio Zn:O [24, 45].

**Figure 4** shows a relatively simple transformation of a metal hydroxide to a metal oxide, by dehydroxylation of Wülfingite only Wurtzite can be obtained; in the scientific literature, there is a very extensive information on the relative simplicity of this transformation, this time a temperature of 600 °C is a maximum referent, but it is known that depending on the synthesis techniques this temperature can be reduced to promote a smaller crystal growth, as well as contribute to decrease the possible secondary processes at low temperatures this is between about 90 and 250 °C.

The interest in ZnO and its application as an anode in lithium-ion batteries is due to its great theoretical capacity ( $987 \text{ mAhg}^{-1}$ ) [25], this with respect to graphite that has a theoretical capacity of around  $372 \text{ mAhg}^{-1}$ , which is the most commonly used material as an anode in lithium batteries [46]. In addition, its theoretical capacity puts it ahead of other transition metals such as Cu, Ni, Fe, or Ti, and even on the Sn of group IV, where there are elements such as Ge and Si of greater theoretical capacities but that have certain disadvantages in terms of their relatively complex synthesis processes and in the case of Ge, rarity and toxicity [47].

Si is the material with the highest theoretical capacity ( $4200 \text{ mAhg}^{-1}$ ); however, one of the big problems is that in a few cycles (10 cycles), it loses its capacity until  $200 \text{ mAhg}^{-1}$ , due to the great volumetric expansion it undergoes in the lithiation process ( $\sim 400\%$ ) [47]. Similarly, ZnO undergoes volumetric changes of  $\sim 228\%$ , which is reflected in a decrease in its efficiency and capacity to  $\sim 400 \text{ mAhg}^{-1}$ ; however, the ZnO has the novelty of having a wide variety of synthesis processes, morphologies, and structures that could help solve these problems [20, 48] as shown in **Figure 4**.

The solution to these problems has motivated several research groups that have chosen to perform CM of ZnO with a great variety of carbonaceous materials, graphite [25], nanotubes [21], or graphene [32, 35, 49, 50]. When using carbonaceous materials, two problems with ZnO are compensated: the low electrical conductivity and as a buffer for the volumetric changes of ZnO [48, 50].

## 2.2 Graphene

Graphene is a crystalline, two-dimensional (2D) material of a single atom in thickness, with covalent bonds  $\sigma$ ,  $sp^2$  between carbon and carbon, with a junction

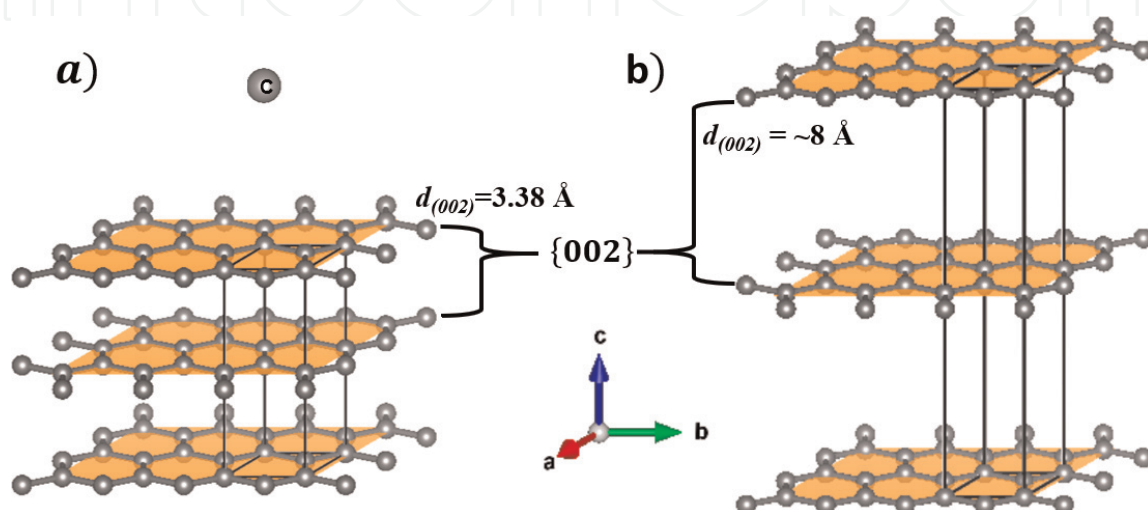


**Figure 5.**  
Crystal structure of (a) graphite and (b) after the oxidation process, a structure equivalent to the GO.



angle of  $120^\circ$  and a length of  $a = 0.14$  nm, resulting in a hexagonal honeycomb lattice, which can be simplified to a trigonal unit cell with two atoms per unit, as shown in **Figure 5**.

Graphene can have other allotropic forms at the same time, since it is the basic building structure of the other forms such as graphite (3D), nanotubes (1D), and fullerenes (0D). In all its structures, it has very good properties of thermal, electrical, and other properties such as mechanical, optical, and magnetic properties. The movement of electrons through a sheet of graphene is governed mainly by the relativistic law of Dirac. For a perfect sheet of graphene, it is estimated that its conductivity reaches  $200,000 \text{ cm}^2/\text{Vs}$ ; however, this intrinsic property is greatly affected by defects that generate dispersion centers generated mainly by substrates, dopants, and chirality.

Since the nineteenth century, oxidized graphite has been produced by different methods: the Brodie method in 1859 [51], the Hummers method in 1958 [52], and the Hummers method modified in July 2004; and in October of the same year, Andre Geim and Kostya Novoselov, professors at the University of Manchester, London, managed to isolate a sheet of graphite a few atoms thick, by mechanical exfoliation, from which they discovered the exceptional properties of this material that has attracted enormous attention since then [53]. However, the synthesis of graphene remains a great challenge, since, to be considered high purity, it is necessary to take into account certain characteristics such as the quality, size, quantity, complexity, and control of the synthesis method. For this reason, it is very important to know the different methods, degrees of purity, and qualities expected for graphene [54]. In the work presented by Hirata et al. [55], they obtained sheets of several nanometers thick and  $20 \mu\text{m}$  wide on average. In the same work, they propose several categories of graphene: oxidized graphene, reduced graphene, functionalized graphene, and graphene in its pure state.

### 3. Methods of synthesis of ZnO

The most used synthesis processes for ZnO are chemical precipitation at normal conditions, synthesis by hydrothermal, solvothermal techniques, and the sol-gel method. The advantage and novelty of these techniques is the obtaining of a great diversity of geometries, with relatively simple processes and with very accessible precursors.

#### 3.1 Chemical precipitation at normal conditions

The technique is used specifically for ZnO, part of a Zn precursor, normally a salt or inorganic compound, soluble in water commonly and as a reducing agent either an acid or a base, which, when reacting in solution with the salt, will form a precipitate or solid of insoluble that will commonly require a calcination process for crystallization. This type of reactions could be expressed in a general equation in the following way:



This type of reactions usually occurs between ionic compounds where one of the products is insoluble, and because each component exchanges pairs, these types of reactions are usually called double-displacement reactions.

Several authors such as Kundu et al. [20] and Liu et al. [48] obtained from chemical precipitation at normal conditions nanobars and ZnO nanoparticles, respectively. According to these same authors, they obtained the nanoparticles or nanobars individually or separately, and in the case of Lui et al. [48], they performed an extra process of carbon coating or as Giri et al. [28] who performed a hydrothermal procedure to coat the nanoparticles. On the other hand, Ramadoss et al. [32] obtained an CM where they precipitated nanoparticles of ZnO in situ, on graphene sheets.

### **3.2 Hydrothermal method**

The method or technique of hydrothermal synthesis is one of the most used for the synthesis of ZnO, and with the same principle of the technique of chemical precipitation, this technique gets its name because the conditions of synthesis, which is carried out in water and temperatures above 25 °C up to ~ 430 °C, reaching autogenous pressures of over 221 bar at ~375 °C, which is the critical point where the liquid phase and gas are not distinguished from water [56]. This type of synthesis is also governed by the precipitation equation but adding temperature and pressure variables.

In various works such as that of Alver et al. [40], they synthesized ZnO doped with boron by the hydrothermal method and subsequently formed a nanocomposite with graphene using the same technique. Yoo et al. [41] with the same method obtained hemispherical nanoparticles of ~25 nm. Wang et al. [57] synthesized ZnO in flower form, doped with Mn, with the hydrothermal method. Bøjesen et al. [36] conducted an in situ study of the growth of ZnO nanoparticles by hydrothermal synthesis. In this work, they conclude that temperature is one of the biggest factors that influences the size and shape characteristics of glass, this, without forgetting other factors such as time.

### **3.3 Solvothermal method**

The solvothermal synthesis method is a variant of the hydrothermal one, since, in this technique, solvents different to water are used, but with the same principles of hydrothermal synthesis and governed by the precipitation equation. The said solvents can be alcohols, acids, bases, or mixtures, since, with this, a greater dissolution or changes in the pressures generated in the synthesis are sought [56]. With the solvothermal synthesis technique, authors such as Wi et al. [19] and Wang et al. [42] have obtained nanoparticle agglomerates, of spherical shape and porous sheet type, respectively. In the case of Wang et al. [42], the synthesis process was carried out at room temperature reaching thicknesses of up to 10 nm in the sheets.

### **3.4 Sol-gel**

On the other hand, the sol-gel synthesis technique consists of a chemical synthesis in which, from a colloidal solution or “sol”, small precipitates of a solid phase gradually form inside a continuous network called “gel”. The peculiarity of the technique is the nanometric size of the particles that can be obtained by this technique as shown in the work of Spanhel et al. [32], who obtained ZnO nanoparticles of colloidal sizes between 3 and 6 nm. Hjiri et al. [33] obtained sizes between 20 and 40 nm for ZnO and up to 3 nm for ZnO doped with Al. Li et al. [34] used the technique to obtain in situ a nanocomposite of nanoparticles deposited in sheets of graphene, whose reported particle size was an average of ~9 nm.

## 4. Graphene synthesis methods

To date, various synthesis methods have been developed for graphene, but basically, there are only two ways: one of them is to obtain the sheets of an existing crystal of graphite which is known as exfoliation methods, and on the other hand, the sheets of graphene can be grown directly on a substrate.

### 4.1 Exfoliation

The exfoliation methods can be classified in two: the micromechanical exfoliation method and the chemical methods, the latter can be by dispersion or oxidation. According to what was reported by Novoselov et al. [53], they used the technique of micromechanical exfoliation, obtaining sheets of graphene up to a single layer; however, this technique is relatively complex, and the yield or number of sheets is very low.

The dispersion method allows obtaining a greater amount of graphene and higher quality than the micromechanical exfoliation. The synthesis of graphene by oxidation is similar to that of dispersion since it is also in the liquid phase, but the graphene that is obtained is of a slightly lower quality, and this is because the GO has a large amount of defects and oxygen at the edges compared to the pristine [54, 57]. To improve the quality of the GO, it can undergo reduction processes and improve the quality of the graphene sheets, obtaining what was called reduced graphene sheets (rG) [54].

The method of Hummers and Offeman [52], reported since 1958, is a method to obtain large quantities of what they called oxidized graphite; in 2004, Hirata et al. [55] modified this method obtaining thinner sheets of better quality. To be reduced, either by heat treatments or chemical means, you can decrease the amounts of oxygen or eliminate it completely under certain conditions. By eliminating oxygen, the graphene sheets increase considerably their electrical conductivity, since the  $sp^3$  bonds decrease while the  $sp^2$  bonds increase, which attribute the excellent properties to graphene. The GO has defects associated with oxygen bonds, at the edges as well as within the plane, forming different functional groups as carbonyls ( $C=O$ ), hydroxyls ( $-OH$ ), and epoxy groups ( $-O-$ ); in **Figure 6** a representative scheme of the structure of a GO sheet is shown; this model was proposed by Santos et al. [59] In addition, this method allowed the production of graphene at higher

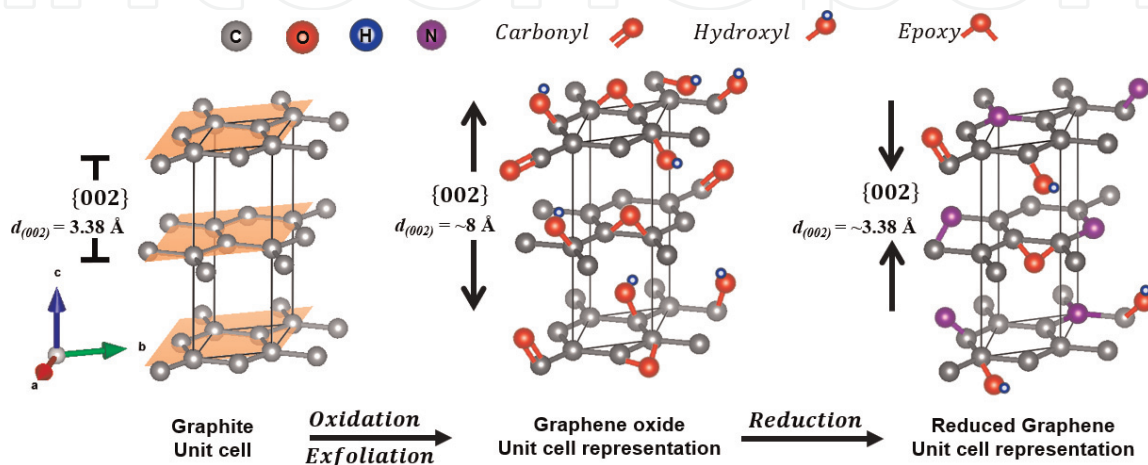


**Figure 6.** Insertion or formation of functional groups in the sheets of graphene.

quantities and the possibility of being used industrially in different carbon products, one of which being Li-ion batteries [58, 59].

The modified Hummers method is currently one of the most used to obtain graphene, due to the sufficient quantity and the relative ease of the process, that once the GO is reduced, its properties are very favored, so that different groups of work have pointed their investigations using this technique to obtain graphene with applications for the anode of Li-ion batteries [61–63].

The Hummers method modified for the synthesis of graphene consists in exposing the graphite particles to prolonged times of combined oxidation to washing and purification processes. The process of Hirata et al. [55] is described as follows: 10 g of natural graphite (99.97 % purity and 24  $\mu\text{m}$  particle diameter) and 7.5 g of  $\text{NaNO}_3$  (99 % purity) were added to a flask. Then 621 g of  $\text{H}_2\text{SO}_4$  (96 %) were added and kept stirring while it was cooled in an ice water bath. Next 45 g of  $\text{KMnO}_4$  (99 %, purity) were added and gradually added over 1 h. The cooling was reached after 2 h, and the mixture remained for 5 days under constant agitation at 20 °C to obtain a highly viscous liquid.

The cleaning and purification process was carried out in the following way; to the obtained liquid, 1 L of solution with 5 % of  $\text{H}_2\text{SO}_4$  was added during 1 h, while it was maintained in agitation, and the obtained mixture in the end was agitated during 2 h more. Then 30 g of  $\text{H}_2\text{O}_2$  (30 % by weight solution) were added and kept under stirring for 2 h and finally separated by centrifugation. This process was repeated 15 times, for the removal of the ions originated in the oxidation process. The synthesis process used by Vargas et al. [64] has modifications such as the change in the use of  $\text{NaNO}_3$  by  $\text{HNO}_3$  and some modifications in synthesis and cleaning methodology. The process they used was the following: 2 g of graphite powder was added to an aqueous solution with 120 mL of  $\text{H}_2\text{SO}_4$  and 80 mL of  $\text{HNO}_3$  in an ice water bath. Then, 10 g of  $\text{KMnO}_4$  was added slowly and remained in reaction for 2 h, during which the temperature remained around 35 °C. The dark brown suspension obtained was diluted with 400 mL of deionized water and turned dark yellow, to then add 8.6 mL of  $\text{H}_2\text{O}_2$  (35 %). A dark brown gel was obtained, after washing with 100 mL of a 10 % solution of HCl and neutral pH obtained after several cycles of washing and centrifugation. The GO was finally obtained by vacuum drying at 80 °C.

Wan et al. [65] synthesized graphene using the modified Hummers method by applying the following process: 1 g of natural graphite was placed in a mixture with a concentrated solution of  $\text{H}_2\text{SO}_4$  (98 %, 92 mL) and concentrated  $\text{HNO}_3$  (65 %, 24 mL) while stirring in an ice water bath, as a safety measure and maintaining the temperature below 10 °C. Then 6 g of  $\text{KMnO}_4$  was added to the solution gradually so that the temperature of the solution did not exceed 20 °C; then the solution was left for 2 h in the ice water bath. Then a temperature controller was used for water flow, to maintain the temperature at 35 °C for 30 min. Subsequently, the temperature was maintained at 85 °C for 30 min. About 100 mL of deionized water was slowly added to the solution, and the temperature was again maintained at 85 °C for 30 min, until a bright yellow product was obtained. After cooling to room temperature and diluting with 10 mL of 30 %  $\text{H}_2\text{O}_2$ . The solution was centrifuged, washed with 1 L of deionized water and a 1:10 HCl solution (1 L) to remove the remaining metal ions, and finally dried at 50 °C and vacuum for 12 h.

Of the three processes described above, the modified Hummers method differs in several aspects of the process such as the change of  $\text{NaNO}_3$  by  $\text{HNO}_3$  and the increase in temperature to reduce the oxidation time, as well as the optimization of the process of cleaning and obtaining the GO. According to the results obtained in what was reported by Wan et al. [65], they obtained GO of five sheets of thickness, with very promising results in the electrochemical tests they carried out.

## 4.2 Substrate growth

This is a totally different way to the previous methods since the graphene sheets can be grown directly on a surface. And the size of the sheets does not depend directly on the size of a graphite crystal, as in the exfoliation methods. Growth can occur in two ways: whether the carbon exists on the surface of the substrate or it is added by chemical vapor deposition (CVD). Graphene can be obtained simply by heating and cooling a silicon carbide crystal, under suitable conditions, obtaining sheets up to a single layer [54].

The chemical vapor deposition method is perhaps one of the most promising and relatively low-cost techniques to obtain good quality graphene. Broadly speaking, the technique consists in the deposition of a solid film on a substrate, where the chemical species of the material deposited come from species in vapor phase and are deposited through chemical reactions. In an ideal CVD process, the transport kinetics of gases is often complicated and complex, since convection and diffusion phenomena occur in different regions of a reactor [66].

The process for obtaining graphene by CVD can be divided into two stages: the first is the pyrolysis of the carbon precursor and the second the formation of the graphene structure. In an ideal synthesis to obtain graphene, temperatures of up to 2500 °C would be needed to overcome the energy barrier that allows the reaction on the surface of the substrate; for this reason, catalysts are used, which are mostly elemental metals, which contribute to the pyrolyzation of carbon precursors. One of the most used substrates is Ni (111) since it has a structure very similar to that of graphene, with a mismatch in network parameters of 1.3 % [54, 64].

The CVD process, as previously described, is a relatively complex process because of the equipment necessary to carry out the synthesis, but it allows obtaining graphene of higher quality at low cost, with larger sizes and more complex forms than the exfoliation processes of graphite [54, 57, 65, 66]. The team of Kim et al. [67] was among the first to report obtaining graphene by the CVD method on a Ni substrate, proving that the monolayers obtained were of much better quality than those of exfoliation. Since then, several authors have continued research to improve the technique, either by lowering the synthesis temperature as reported by Jang et al. [68], who obtained graphene at temperatures between 100 and 300 °C deposited on copper sheets, using benzene. Other authors such as Sagar et al. [58] have synthesized highly porous structures based on interconnected sheets of graphene and have proposed an anode in Li-ion batteries.

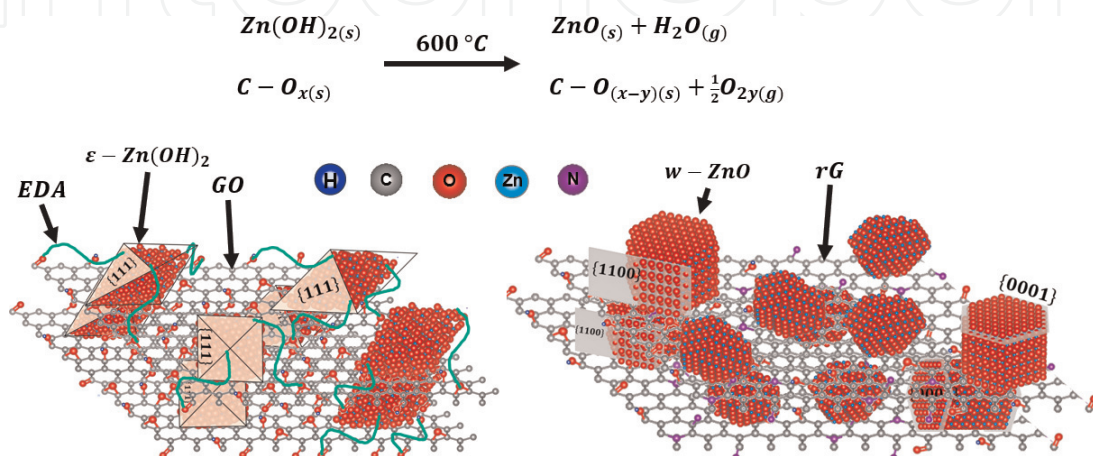


**Figure 7.** Scheme of obtaining the MC type ZnO-rG. Left: material of the precursor phase  $\text{Zn(OH)}_2$ -GO. Right: the MC ZnO-rG obtained after a thermal treatment at 600 °C.

### 4.3 Composite ZnO-graphene materials

An CM of ZnO-graphene (ZnO-G) could have a large number of assembly structures, however, can be considered six principally, the most used in this type of CM for Li-ion batteries: (a) anchored, (b) wrapped, (c) encapsulated, (d) type sandwich, (e) laminar, and (f) mixed. In all cases, graphene, being a two-dimensional material, is the one that functions as a support for dispersed nanoparticles whose three-dimensional morphology can vary in different sizes, shapes, and crystallinity [13, 66].

Currently, the CM based on ZnO and carbon are very diverse and with variations in the morphology of both phases of the components. **Figure 7** shows the obtaining of an CM of possible interest with the specific case of obtaining the dispersed phase of the phases of the ZnO with a Wurtzite type crystal structure, whose structure is more stable to standard conditions; this phase is the most attractive for, it is mainly used in CM for Li-ion batteries, also presented with a wide variety of morphologies; while for graphene, it usually presents different characteristics and properties according to its synthesis method [25, 69].

In recent years, a great amount of research has been carried out regarding the morphology of ZnO, since most of these works seek to increase the area, modifying the morphology and thus increasing the electrochemical properties, for its application in Li-ion batteries [16]. The investigations that have been carried out regarding the control of the crystallinity in the particles of the ZnO, to increase the capacity, are very few. Recently Mei et al. [17] published a paper in which they analyzed the degree of crystallinity and structural patterns of ZnO as an anode in Li-ion batteries. In this work, they used the hydrothermal synthesis in which they modified concentrations, to obtain different morphologies and then carried out treatments at different temperatures, this to control the degree of crystallinity. Finally, Mei et al. concluded that morphology was an important part in the capacity, since certain morphologies present a greater quantity of internal spaces, which help to compensate the volumetric changes; however, the samples whose crystallinity was controlled presented a specific capacity of 1328 mAhg<sup>-1</sup> in the first cycle and 663 mAhg<sup>-1</sup> at 50 cycles. In this work, it is worth mentioning that the particles obtained are of the micrometric order, contrary to what is generally reported with nanometric materials, such as Li et al. [18] that dispersed ZnO nanoparticles in

Morphology	Reversible capacity (mAhg <sup>-1</sup> )	Number of cycles	Ref.
Microparticles distributed radially	320	100	[6]
Nanobars	310	40	[20]
Microbars	663	50	[17]
Nanoplates	400	100	[25]
Nanoplates	421	100	[25]
Nanoparticles	318	100	[42]
Flower type	662	50	[17]
Spheres	109	100	[70]
Cluster	800	50	[71]
Microbars	811	80	[72]
Nanoparticles	318	100	[73]

**Table 2.**  
 Electrochemical characteristics of ZnO applied as an anode material in Li-ion batteries.

graphene, obtaining an initial capacity of  $1652 \text{ mAhg}^{-1}$ , but the retention capacity decreased to  $318 \text{ mAhg}^{-1}$ .

**Table 2** shows the data reported in the literature for the comparison of the reversible capacity and the number of cycles of the different morphologies of ZnO as an anode in Li-ion batteries. It is possible to identify the effect of each morphology in the particle of the ZnO; the geometry of the bars is distinguished from the others, because it presents a greater reversible capacity, which suggests a greater stability in the processes of lithiation and sliding. In **Table 2**, it can be seen that some reversible capacity values greater or closer to  $600 \text{ mAhg}^{-1}$ , the ZnO particles are CM shaped with a carbonaceous material. However, the value of  $663 \text{ mAhg}^{-1}$  of the microbars reported by Mei et al. It is of great interest, because in spite of not being of nanometric size and not being like CM it has a great reversible capacity.

The ZnO-rG CMs promise better results due to the good properties of graphene. **Table 2** shows results of some CMs of ZnO with carbon, porous carbon, graphite,

Method	Initial capacity ( $\text{mAhg}^{-1}$ )	Reversible capacity ( $\text{mAhg}^{-1}$ )	Number of cycles	Ref.
Rapid exfoliation at $1050 \text{ }^\circ\text{C}/\text{N}_2$	2000	1200	5	[64]
Exfoliation $300 \text{ }^\circ\text{C}/\text{Ar}$	2100	600	100	[64]
Reduction with autoclaved $\text{N}_2\text{H}_4$ (DODA-Br)	3000	1100	50	[64]
Fast exfoliation at $1050 \text{ }^\circ\text{C}/\text{Ar}$	2035	848	40	[5]
Exfoliation at $300 \text{ }^\circ\text{C}/\text{Ar}$	2137	478	100	[65]
Thermal reduction exfoliation	1480	500	60	[74]
Thermal reduction exfoliation/ $\text{N}_2$	3250	1354	50	[75]

**Table 3.**  
*Electrochemical characteristics of graphene in Li-ion batteries.*

CM	Reversible capacity ( $\text{mAhg}^{-1}$ )	Number of cycles	Ref.
ZnO/G	516	100	[35]
ZnO/GN	1100	100	[50]
AZO/G	391	100	[49]
ZnO/G	360	200	[76]
ZnO/G	550	100	[77]
ZnO/G	560	100	[78]
ZnO/G	300	50	[79]
ZnO/CN	1047	100	[80]
ZnO/G	749	100	[81]
ZnO/G	550	100	[82]
Cu/ZnO/G	630	100	[83]
ZnO/C	520	100	[84]
ZnO/CN	1177	100	[85]
ZnO/NSG	720	100	[73]

NC = nitrated carbon; G = graphene; NG = nitrated graphene; NSG = nitrated-sulfurized graphene.

**Table 4.**  
*Electrochemical characteristics of an CM of ZnO-G in Li-ion batteries.*

and graphene, of which graphene, in this case, is reduced with nitrogen and showed a very remarkable reversible capacity, comparing it with other results. The graphene used in most CMs is obtained by chemical exfoliation, called GO, which has a number of advantages with pristine-type graphene. The GO can be obtained in large quantities and of sufficient quality, using the modified Hummers method, to be used in CM in a large number of applications, as in Li-ion batteries [5, 54].

The high area and the conductivity properties of graphene are the main properties that call attention to this material to be used as an anode in Li-ion batteries. The first reported evidence of Li storage on a large scale was  $500 \text{ mAhg}^{-1}$  for the first cycle and  $300 \text{ mAhg}^{-1}$  at just 20 cycles; currently values of up to  $3000 \text{ mAhg}^{-1}$  have been reported for the first cycle and decrements to values of  $200 \text{ mAhg}^{-1}$  after a few cycles [64]. **Table 3** shows some data of the reported GO properties by different reduction methods. It should be mentioned that the GO of the data in **Table 3** was obtained by the modified Hummers method.

When analyzing the data in **Table 4**, it is observed that the efficiency or loss of capacity in graphene is notoriously greater due to the formation of the SEI; furthermore, it is observed that the GO reduced by thermal treatments, under an argon atmosphere, it has the best reversible capabilities and a greater number of cycles. The recently published ZnO-rG CMs are based on a reduced GO afterward and in which the ZnO nanoparticles are deposited or grow in situ in the leaves. In **Table 4**, some relevant values of CM of ZnO-rG are shown, in which the ZnO particles are of the order of hemispherical nanoparticles. Now, by comparing the values of the reversible capacity, it can be seen that they are close to  $500 \text{ mAhg}^{-1}$  on an average of per 100 cycles. The data reported in the literature for ZnO-G composites have very low efficiencies of around 50 %, however, some reports such as that of Dai et al. [50], Eliana et al. [25], and Shen et al. [43] have reported values very close to the theoretical capacity.

The efficiency problems that currently arise in the materials for Li-ion battery anodes are mainly due to the pulverization and fragmentation of the said materials, caused by the volumetric changes and stability problems during the charge/discharge cycles. On the other hand, one of the factors that remain unfinished for this type of CMs is the surface interaction between graphene and MO that during the charge and discharge cycles is affected by parasitic reactions that impede the stability and diffusion of charges between both materials [13, 66].

## 5. Conclusions

The evidences reported in the scientific literature show an open thematic for the design of composite materials with the intention of directly impacting on this time of tool for the storage of electrochemical energy, being the ZnO-graphene system a great candidate to be used as a constituent material of the anode.

## Acknowledgements

The authors are grateful for the support granted in the Call 2019 issued by the Program of Support for Scientific and Technological Research in the Educational Programs of the Federal, Decentralized Technological Institutes and Centers belonging to the National Technological of Mexico (TecNM) for the support assigned to the Project (5269.19-P); and to the Higher Technological Institute of Irapuato (ITESI) for the allocation of support from its Institutional Program for the Strengthening of Academic Staff (PIFOCA/PIFOPA/PIICYT 2019).



IntechOpen

### **Author details**

Herrera-Pérez Gabriel<sup>1\*</sup>, Pérez-Zúñiga Germán<sup>2</sup>, Verde-Gómez Ysmael<sup>2</sup>,  
Valenzuela-Muñiz Ana María<sup>2</sup> and Vargas-Bernal Rafael<sup>1</sup>

1 Department of Materials Engineering, Higher Technological Institute of Irapuato, Guanajuato, Mexico

2 Postgraduate Studies and Research Division, Technological Institute of Cancún, Quintana Roo, Mexico

\*Address all correspondence to: gaherrera@itesi.edu.mx

### **IntechOpen**

---

© 2019 The Author(s). Licensee IntechOpen. This chapter is distributed under the terms of the Creative Commons Attribution License (<http://creativecommons.org/licenses/by/3.0>), which permits unrestricted use, distribution, and reproduction in any medium, provided the original work is properly cited. 

## References

- [1] Scrosati B, Garche J. Lithium batteries: Status, prospects and future. *Journal of Power Sources*. 2010;**195**: 2419-2430
- [2] Trasatti S. 1799–1999: Alessandro Volta's 'electric pile. *Journal of Electroanalytical Chemistry*. 1999;**460** (1–2):1-4
- [3] Kurzweil P. Gaston Planté and his invention of the lead-acid battery-the genesis of the first practical rechargeable battery. *Journal of Power Sources*. 2010;**195**(14):4424-4434
- [4] Armand M, Tarascon J-M. Building better batteries. *Nature*. 2008; **451**(7179):652-657
- [5] Lockwood JD. *Nanotechnology for Lithium-Ion Batteries*. Boston, MA: Springer, US; 2013
- [6] Amine K, Kanno R, Tzeng Y. Rechargeable lithium batteries and beyond: Progress, challenges, and future directions. *MRS Bulletin*. 2014;**39**(5): 395-401
- [7] Robinson AL, Janek J. Solid-state batteries enter EV fray. *MRS Bulletin*. 2014;**39**(12):1046-1047
- [8] Linden D, Reddy T. *Handbook of Batteries*, 3rd ed.; 2001
- [9] Park M, Zhang X, Chung M, Less GB, Sastry AM. A review of conduction phenomena in Li-ion batteries. *Journal of Power Sources*. 2010;**195**(24): 7904-7929
- [10] Gon J, Son B, Mukherjee S, Schuppert N, Bates A, Kwon O, et al. A review of lithium and non-lithium based solid state batteries. *Journal of Power Sources*. 2015;**282**:299-322
- [11] Armstrong MJ, O'Dwyer C, Macklin WJ, Holmes JD. Evaluating the performance of nanostructured materials as lithium-ion battery electrodes. *Nano Research*. 2014;**7**(1): 1-62
- [12] Fan X, Zheng WT, Kuo JL, Singh DJ. Adsorption of single Li and the formation of small Li clusters on graphene for the anode of lithium-ion batteries. *ACS Applied Materials & Interfaces*. 2013;**5**(16):7793-7797
- [13] Mazar Atabaki M, Kovacevic R. Graphene composites as anode materials in lithium-ion batteries. *Electronic Materials Letters*. 2013;**9**(2):133-153
- [14] Dahn JR, Zheng T, Liu Y, Xue JS. Mechanisms for Lithium insertion in carbonaceous materials. *Science*. 1995; **270**(5236):590-593
- [15] Tarascon J, Poizot P, Laruelle S, Grugeon S, Dupont L. Nano-sized transition-metal oxides as negative-electrode materials for lithium-ion batteries. *Nature*. 2000;**407**(6803): 496-499
- [16] Yuan GH, Wang G, Wang H, Bai JT. Synthesis and electrochemical investigation of radial ZnO microparticles as anode materials for lithium-ion batteries. *Ionics (Kiel)*. 2015;**21**(2):365-371
- [17] Xiao L, Mei D, Cao M, Qu D, Deng B. Effects of structural patterns and degree of crystallinity on the performance of nanostructured ZnO as anode material for lithium-ion batteries. *Journal of Alloys and Compounds*. 2015; **627**:455-462
- [18] Li H, Wei Y, Zhang Y, Yin F, Zhang C, Wang G, et al. Synthesis and electrochemical investigation of highly dispersed ZnO nanoparticles as anode material for lithium-ion batteries. *Ionics (Kiel)*. 2016;**22**(8):1387-1393

- [19] Wi S, Woo H, Lee S, Kang J, Kim J, An S, et al. Reduced graphene oxide/carbon double-coated 3-D porous ZnO aggregates as high-performance Li-ion anode materials. *Nanoscale Research Letters*. 2015;**10**:1-8
- [20] Kundu S, Sain S, Yoshio M, Kar T, Gunawardhana N, Pradhan SK. Structural interpretation of chemically synthesized ZnO nanorod and its application in lithium ion battery. *Applied Surface Science*. 2015;**329**: 206-211
- [21] Guler MO, Cetinkaya T, Tocoglu U, Akbulut H. Electrochemical performance of MWCNT reinforced ZnO anodes for Li-ion batteries. *Microelectronic Engineering*. 2014;**118**: 54-60
- [22] Wróbel J, Piechota J. On the structural stability of ZnO phases. *Solid State Communications*. 2008;**146**(7-8): 324-329
- [23] Meulenkamp EA. Synthesis and growth of ZnO nanoparticles. *The Journal of Physical Chemistry. B*. 1998; **5647**(98):5566-5572
- [24] Wang ZL. Zinc oxide nanostructures: Growth, properties and applications. *Journal of Physics. Condensed Matter*. 2004;**16**: R829-R858
- [25] Quartarone E, Asta VD, Resmini A, Tealdi C, Tredici IG, Tamburini UA, et al. Graphite-coated ZnO nanosheets as high-capacity, highly stable, and binder-free anodes for lithium-ion batteries. *Journal of Power Sources*. 2016;**320**:314-321
- [26] Zhang L, Zhao J, Lu H, Li L, Zheng J, Li H, et al. Facile synthesis and ultrahigh ethanol response of hierarchically porous ZnO nanosheets. *Sensors and Actuators B: Chemical*. 2012;**161**(1):209-215
- [27] Yue H, Shi Z, Wang Q, Cao Z, Dong H, Qiao Y, et al. MOF-derived cobalt-doped ZnO@C composites as a high-performance anode material for lithium-ion batteries. *ACS Applied Materials & Interfaces*. 2014;**6**(19): 17067-17074
- [28] Giri A, Pal P, Ananthakumar R, Jayachandran M, Mahanty S, Panda A. 3D hierarchically assembled porous wrinkled paper-like structure of ZnCo<sub>2</sub>O<sub>4</sub> and Co-ZnO@C as anode materials for lithium-ion batteries. *Crystal Growth & Design*. 2014;**14**: 3352-3359
- [29] Søndergaard M, Bøjesen ED, Christensen M, Iversen BB. Supporting information size and morphology dependence of ZnO nanoparticles synthesized by a fast continuous flow hydrothermal method. *Crystal Growth & Design*. 2011;**11**(9):4027-4033
- [30] Sun Y, Yang GZ, Cui H, Wang J, Wang CX. Zn<sub>x</sub>Ge<sub>1-x</sub>O 3D micronano structures with excellent performance as anode material in Lithium ion battery. *ACS Applied Materials & Interfaces*. 2015;**7**(28): 15230-15239
- [31] Heo YW et al. ZnO nanowire growth and devices. *Materials Science and Engineering R: Reports*. 2004; **47**(1-2):1-47
- [32] Ramadoss A, Kim SJ. Facile preparation and electrochemical characterization of graphene/ZnO nanocomposite for supercapacitor applications. *Materials Chemistry and Physics*. 2013;**140**(1):405-411
- [33] Spanhel L, Anderson MA. Semiconductor clusters in the sol-gel process: Quantized aggregation, gelation, and crystal growth in concentrated ZnO colloids. *Journal of the American Chemical Society*. 1991; **113**:2826-2833

- [34] Hjiri M, El Mir L, Leonardi SG, Pistone A, Mavilia L, Neri G. Al-doped ZnO for highly sensitive CO gas sensors. *Sensors and Actuators B: Chemical*. 2014;**196**:413-420
- [35] Li H, Wei Y, Zhang Y, Zhang C, Wang G, Zhao Y, et al. In situ sol-gel synthesis of ultrafine ZnO nanocrystals anchored on graphene as anode material for lithium-ion batteries. *Ceramics International*. 2016:1-8
- [36] Bøjesen ED, Jensen KMØ, Tyrsted C, Lock N, Christensen M, Iversen BB. In situ powder diffraction study of the hydrothermal synthesis of ZnO nanoparticles. *Crystal Growth & Design*. 2014;**14**: 2803-2810
- [37] Demoisson F, Piolet R, Bernard F. Hydrothermal growth of ZnO nanostructures in supercritical domain: Effect of the metal salt concentration ( $Zn(NO_3)_2$ ) in alkali medium (KOH). *Journal of Supercritical Fluids*. 2015;**97**: 268-274
- [38] Wang R, Wu SP, Lv YC, Lin ZQ. Partially crystalline  $Zn_2GeO_4$  nanorod/graphene composites as anode materials for high performance Lithium ion batteries. *Langmuir*. 2014;**30**(27): 8215-8220
- [39] Bai S, Guo T, Zhao Y, Sun J, Li D, Chen A, et al. Sensing performance and mechanism of Fe-doped ZnO microflowers. *Sensors and Actuators B: Chemical*. 2014;**195**(3):657-666
- [40] Alver Ü, Tanriverdi A. Boron doped ZnO embedded into reduced graphene oxide for electrochemical supercapacitors. *Applied Surface Science*. 2016;**378**:368-374
- [41] Yoo R, Cho S, Song MJ, Lee W. Highly sensitive gas sensor based on Al-doped ZnO nanoparticles for detection of dimethyl methylphosphonate as a chemical warfare agent simulant. *Sensors and Actuators B: Chemical*. 2015;**221**:217-223
- [42] Wang X, Huang L, Zhao Y, Zhang Y, Zhou G. Synthesis of mesoporous ZnO nanosheets via facile solvothermal method as the anode materials for Lithium-ion batteries. *Nanoscale Research Letters*. 2016;**11**(1):37
- [43] Shen X, Mu D, Chen S, Wu B, Wu F. Enhanced electrochemical performance of ZnO-loaded/porous carbon composite as anode materials for lithium ion batteries. *ACS Applied Materials & Interfaces*. 2013;**5**(8): 3118-3125
- [44] Azzaz Y, Kacimi S, Zaoui A, Bouhafs B. Electronic properties and stability of ZnO from computational study. *Physica B: Condensed Matter*. 2008;**403**(18): 3154-3158
- [45] Pearton SJ, Norton DP, Ip K, Heo YW, Steiner T. Recent progress in processing and properties of ZnO. *Progress in Materials Science*. 2005;**50**(3):293-340
- [46] Köse H, Dombaycıoğlu Ş, Aydın AO, Akbulut H. Production and characterization of free-standing ZnO/SnO<sub>2</sub>/MWCNT ternary nanocomposite Li-ion battery anode. *International Journal of Hydrogen Energy*. 2016:1-9
- [47] Ma D, Cao Z, Hu A. Si-based anode materials for li-ion batteries: A mini review. *Nano-Micro Letters*. 2014;**6**(4): 347-358
- [48] Liu Y, Li Y, Zhong M, Hu Y, Hu P, Zhu M, et al. A facile synthesis of core-shell structured ZnO@C nanosphere and their high performance for lithium ion battery anode. *Materials Letters*. 2016;**171**:244-247

- [49] Zhang L, Zhang J, Liu Y, Zheng P, Yuan X, Guo S. Al doped-ZnO nanoparticles implanted in reduced graphene oxide with improved electrochemical properties for lithium ion batteries. *Materials Letters*. 2016; **165**:165-168
- [50] Dai J, Wang M, Song M, Li P, Zhang C, Xie A, et al. A novel synthesis of ZnO/N-doped reduced graphene oxide composite as superior anode material for lithium-ion batteries. *SMM*. 2016; **112**:67-70
- [51] Brodie BC. On the atomic weight of graphite. *Philosophical Transactions. Royal Society of London*. 1859; **149**(9): 249-259
- [52] Hummers W, Offeman R. Preparation of grafitic oxide. *Journal of the American Chemical Society*. 1958; **80**(6):1339
- [53] Novoselov KS, Geim AK, Morozov SV, Jiang D, Zhang Y, Dubonos SV, et al. Electric field effect in atomically thin carbon films. *Science*. 2004; **306**(5696): 666-669
- [54] Sattler KD. *Carbon Nanomaterials Sourcebook: Graphene, Fullerenes, Nanotubes, and Nanodiamonds*. Vol. I, 1st ed. CRC Press; 2016
- [55] Hirata M, Gotou T, Horiuchi S, Fujiwara M, Ohba M. Thin-film particles of graphite oxide. 1: High-yield synthesis and flexibility of the particles. *Carbon N. Y.* 2004; **42**(14): 2929-2937
- [56] Ehrentraut D, Sato H, Kagamitani Y, Sato H, Yoshikawa A, Fukuda T. Solvothermal growth of ZnO. *Progress in Crystal Growth and Characterization of Materials*. 2006; **52**(4):280-335
- [57] Wang L, Tang K, Zhang M, Xu J. Facile synthesis of Mn-doped ZnO porous nanosheets as anode materials for lithium ion batteries with a better cycle durability. *Nanoscale Research Letters*. 2015; **3**-7
- [58] Ur R, Sagar R, Mahmood N, Stadler FJ, Anwar T, Navale ST, et al. High capacity retention anode material for lithium ion battery. *Electrochimica Acta*. 2016; **211**:156-163
- [59] Lee DW, De Los Santos VL, Seo JW, Felix LL, Bustamante AD, Cole JM, et al. The structure of graphite oxide: Investigation of its surface chemical groups. *The Journal of Physical Chemistry. B*. 2010; **114**(17):5723-5728
- [60] Park RS, Ruoff S. Chemical methods for the production of graphenes. *Nature Nanotechnology*. 2009; **4**:217-224
- [61] Lu XY, Jin XH, Sun J. Advances of graphene application in electrode materials for lithium ion batteries. *Science China Technological Sciences*. 2015; **58**(11):1829-1840
- [62] Petnikota S, Rotte NK, Srikanth VVSS, Kota BSR, Reddy MV, Loh KP, et al. Electrochemical studies of few-layered graphene as an anode material for Li ion batteries. *Journal of Solid State Electrochemistry*. 2014; **18**(4):941-949
- [63] Shan H, Li X, Cui Y, Xiong D, Yan B, Li D, et al. Sulfur/nitrogen dual-doped porous graphene aerogels enhancing anode performance of lithium ion batteries. *Electrochimica Acta*. 2016; **205**:187-197
- [64] Vargas COA, Caballero Á, Morales J. Can the performance of graphene nanosheets for lithium storage in Li-ion batteries be predicted? *Nanoscale*. 2012; **4**(6):2083-2092
- [65] Wan L, Ren Z, Wang H, Wang G, Tong X, Gao S, et al. Graphene nanosheets based on controlled exfoliation process for enhanced lithium storage in lithium-ion battery. *Diamond and Related Materials*. 2011; **20**(5-6): 756-761

- [66] Miao C, Zheng C, Liang O, Xie Y. Chemical vapor deposition of graphene. In: *Physics and Applications of Graphene—Experiments*. 2011. pp. 37-54
- [67] Kim KS, Zhao Y, Jang H, Lee SY, Kim JM, Kim JM, et al. Large-scale pattern growth of graphene films for stretchable transparent electrodes. *Applied Physics Letters*. 2009;**457**:706-710
- [68] Jang J, Son M, Chung S, Kim K, Cho C, Lee BH, et al. Low-temperature-grown continuous graphene films from benzene by chemical vapor deposition at ambient pressure. *Scientific Reports*. 2015;1-7
- [69] Wu S, Xu R, Lu M, Ge R, Iocozzia J, Han C, et al. Graphene-containing nanomaterials for lithium-ion batteries. *Advanced Energy Materials*. 2015;**5**(21):1-40
- [70] Wu G, Jia Z, Cheng Y, Zhang H, Zhou X. Easy synthesis of multi-shelled ZnO hollow spheres and their conversion into hedgehog-like ZnO hollow spheres with superior rate performance for lithium ion batteries. *Applied Surface Science*. 2019;**464**:472-478
- [71] Yan J et al. Preparation and electrochemical performance of bramble-like ZnO array as anode materials for lithium-ion batteries. *Journal of Nanoparticle Research*. 2015;**17**(1)
- [72] Pambudi YDS, Setiabudy R, Yuwono AH, Kartini E, Lee JK, Hudaya C. Effects of annealing temperature on the electrochemical characteristics of ZnO microrods as anode materials of lithium-ion battery using chemical bath deposition. *Ionics (Kiel)*. 2019;**25**(2):457-466
- [73] Yang C et al. ZnO nanoparticles anchored on nitrogen and sulfur co-doped graphene sheets for lithium-ion batteries applications. *International Journal of Ionics The Science and Technology of Ionic Motion*. 2018;**24**(12):3781-3791
- [74] Chowdari BVR, Srikanth VVSS, Adams S, Puttapati SK, Reddy MV, Gedela V. Unique reduced graphene oxide as efficient anode material in Li ion battery. *Bulletin of Materials Science*. 2018;**41**(2)
- [75] Dong X, Yang Z, Yang W, Wu X, Lu Y. ZnO-templated N-doped holey graphene for efficient lithium ion storage performance. *Materials Chemistry and Physics*. 2018;**205**:487-493
- [76] Wu J, Chen C, Hao Y, Wang C. Enhanced electrochemical performance of nanosheet ZnO/reduced graphene oxide composites as anode for lithium-ion batteries. *Colloids and Surfaces A: Physicochemical and Engineering Aspects*. 2015;**468**:17-21
- [77] Fang H, Zhao L, Yue W, Wang Y, Jiang Y, Zhang Y. Facile and large-scale preparation of sandwich-structured graphene-metal oxide composites as anode materials for Li-ion batteries. *Electrochimica Acta*. 2015;**186**:397-403
- [78] Guo R, Yue W, An Y, Ren Y, Yan X. Graphene-encapsulated porous carbon-ZnO composites as high-performance anode materials for Li-ion batteries. *Electrochimica Acta*. 2014;**135**:161-167
- [79] Hsieh C-T, Lin C-Y, Chen Y-F, Lin J-S. Synthesis of ZnO@graphene composites as anode materials for lithium ion batteries. *Electrochimica Acta*. 2013;**111**:359-365
- [80] Kim H, Jae W, Song J, Kim J. Skein-shaped ZnO/N-doped carbon microstructures as a high performance anode material for lithium-ion batteries. *Journal of Alloys and Compounds*. 2019;**772**:507-515

[81] Feng Y, Zhang Y, Song X, Wei Y, Battaglia VS. Facile hydrothermal fabrication of ZnO-graphene hybrid anode materials with excellent lithium storage properties. *Sustain. Energy Fuels*. 2017;**1**(4):767-779

[82] Qi Y, Zhang Y, Liu C, Zong S, Men Y. Room-temperature synthesis of ZnO @ GO nanocomposites as anode for lithium-ion batteries. *Journal of Materials Research and Technology*. 2018;**33**(10):1506-1514

[83] Jacob L, Prasanna K, Vengatesan MR, Santhoshkumar P, Woo C, Mittal V. Binary Cu/ZnO decorated graphene nanocomposites as an efficient anode for lithium ion batteries. *Journal of Industrial and Engineering Chemistry*. 2018;**59**:108-114

[84] Shen X, Cao Z, Zhang J, Li T, Jiang W. In-situ loading of ZnO nanoparticles on carbon felt as novel binder-free flexible anode for high performance lithium-ion batteries. *Materials Letters*. 2018;**229**:93-97

[85] Kim T, Kim H, Han JM, Kim J. ZnO-embedded N-doped porous carbon nanocomposite as a superior anode material for lithium-ion batteries. *Electrochimica Acta*. 2017;**253**:190-199